Appendix A.21:

15b Royds Pl – VsVp 57326

Table 1: Site Description for 15b Royds Pl (v_sv_p 57326).

Attribute	Yes/No			Description/Date	Symbol in Figure 1
	10-m Buffer	20-m Buffer	50-m Buffer		
Near a body of surface water or other free face features?	No	Yes	Yes	The center of the site is ~10 m away from the Waimairi Stream. The stream runs through all quadrants of the 20-m and 50-m buffers; its height ranges from <0.5 m to ~1.0 m.	Blue line
Lateral spreading observed during the CES?	Yes	Yes	Yes	No lateral spreading was observed for the September 2010 earthquake but the February 2011 earthquake.[1,*]	NA
Nearby buildings or structures?	Yes	Yes	Yes	Building coverage of the 10-m, 20-m, and 50-m buffers is 3%, 23%, and 24%, respectively.	White fill + Brown outline
Sloping land?	No	No	Yes	Predominantly flat, residential area; however, there is a slightly sloping ground toward the stream (primarily in the NE quadrant).	NA
Step changes in the ground surface?	Yes	Yes	Yes	Along the stream.	NA
Retaining walls?	No	No	Yes	Supporting approximately 0.5 m - 1.2 m of soil in height along the stream in all quadrants.	NA
Vegetation?	Yes	Yes	Yes	Trees and bushes cover 49, 50, and 51% of the 10-, 20-, and 50-m buffers. They are in all quadrants of the buffers.	White fill + Green outline
Anthropogenic changes to the site between the LiDAR surveys?	No	No	No	NA	NA
Other important factors?	Yes	Yes	Yes	A swimming pool in the SE and SW quadrants covers 11, 3, and ~0% of the 10-, 20-, and 50-m buffers. A small pedestrian bridge spans the stream in the NE quadrant of the 50-m buffer.	Pool: White fill + Blue outline Bridge: White fill + Orange outline

Note: Buffer is the area within a circle of a specified radius with CPT investigations done at its center (172.603276°, -43.520686°); * indicates that the settlement analysis was conducted only for the September 2011 earthquake due to lateral spreading observed for the February 2011 earthquake (the anthropogenic changes description pertains to the period between Dec 2004 and Feb 2011 only).

[1] Canterbury Geotechnical Database. (2012). "Observed Ground Crack Locations", Map Layer CGD0400 - 23 July 2012, retrieved July 09, 2018 from https://canterburygeotechnicaldatabase.projectorbit.com/

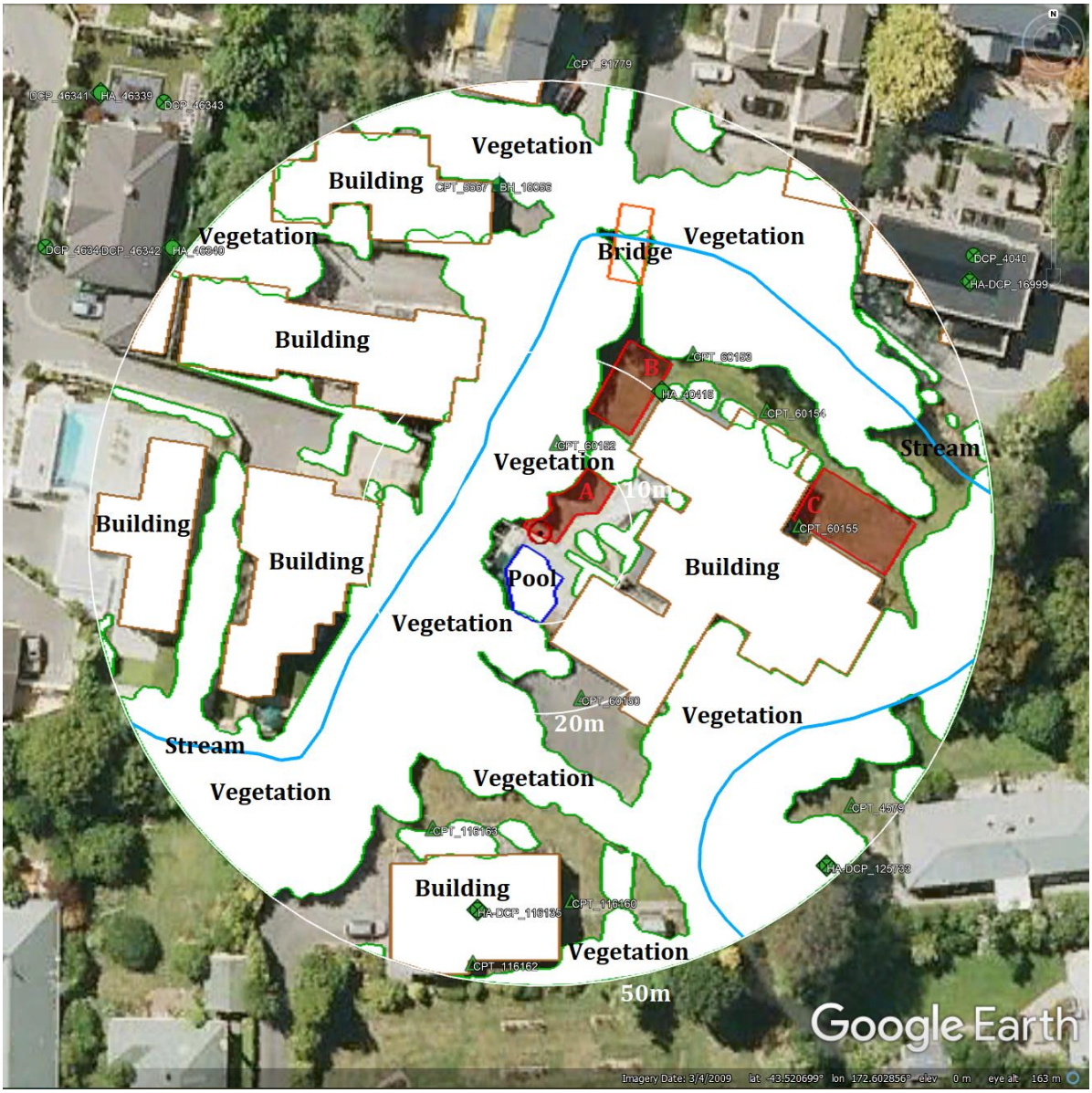

Figure 1: Site plan with areas where ejecta-induced settlement is considered.

Note 1: Three patches (outlined in red) in free field were initially selected for settlement assessment as areas free of vegetation and structures. Further analyses such as proximity of a patch to a CPT, proximity of a patch to a property subjected to addition and/or demolition of a structure and the sloping ground, front yard/backyard alterations (e.g., ploughing, rubble, scrap), and aerial distribution of sediment ejecta resulted in all three patches being selected for detailed settlement assessment.

Table 2: LiDAR flight error adjustments, global adjustments for the difference between average LiDAR point elevations and benchmark survey elevations, and vertical tectonic movement adjustments.

	Adjustments (mm)		
Earthquake Event(s)	LiDAR Flight Error	Global Offset[2]	Tectonic Vertical Movement
Sep-10	NA	-3	0
Feb-11	NA	16	-50
Jun-11	0	38	-20
Dec-11	-100	-65	0
CES	-100	-14	-70
Any 2010 LiDAR survey affected by ejecta?			No

Notes: The negative sign indicates the subtraction from the ground surface subsidence, while the positive sign indicates the addition to the ground surface subsidence; NA = Not available due to the absence of the Sep-10 LiDAR survey.

Table 3: LiDAR Measurement Error for Patches A, B, and C.

Surveys	Buffer	Area Averaged Difference Indicating Repeat Measurement Error (mm)	$\sigma^*_{\text{individual LiDAR points}}$ (mm)	%Reduction in σ due to Area Averaging of LiDAR Points
Post Feb 2011: Mar 2011 and May 2011	10-m	ND	59	[ND,ND]
	20-m	ND		
	50-m	ND		
Post Dec 2011: Feb 2012 and Oct 2015	10-m	ND	70	[ND,ND]
	20-m	ND		
	50-m	ND		

*Standard deviation; ND = Not determined due to lateral spreading.

[2] Russell, J., & van Ballegooy, S. (2015). *Canterbury Earthquake Sequence: Increased liquefaction vulnerability assessment methodology*. New Zealand: Tonkin & Taylor Ltd.

Table 4: Ground surface subsidence adjustments due to LiDAR measurement error for Patches A, B, and C.

Earthquake Event(s)	$\sigma_{\text{pre-EQ LiDAR survey}}$ (mm)	$\sigma_{\text{post-EQ LiDAR survey}}$ (mm)	σ_{total} (mm)	Area Average Adjusted σ (mm) **
Sep-10	158	56	134	±ND
Feb-11	56	59	59	±ND
Jun-11	59	61	62	±ND
Dec-11	61	70	87	±ND
CES	158	70	124	±ND

**Based on the highest %Reduction in Table 3a; ND = Not determined due to lateral spreading.

Table 5: Raw liquefaction-related ground surface subsidence using original LiDAR points for Patches A, B, and C.

	Average Ground Surface Subsidence (mm)		
Earthquake Event(s)	10-m Buffer	20-m Buffer	50-m Buffer
Sep-10	NA	NA	NA
Feb-11	ND	ND	ND
Jun-11	ND	ND	ND
Dec-11	ND	ND	ND
CES	ND	ND	ND

Notes: ND = Not determined due to lateral spreading; ND = Not available due to the absence of the Sep-2010 LiDAR survey.

Table 6: Corrected liquefaction-related ground surface subsidence using original LiDAR points for Patches A, B, and C with the calculated adjustments in Table 2.

	Average Calculated Ground Surface Subsidence (mm)		
Earthquake Event(s)	10-m Buffer	20-m Buffer	50-m Buffer
Sep-10	NA	NA	NA
Feb-11	ND	ND	ND
Jun-11	ND	ND	ND
Dec-11	ND	ND	ND
CES	ND	ND	ND

Notes: Plus/minus values are same as those in Table 4a, but rounded to the nearest 25; Positive overall values indicate ground surface subsidence, while negative overall values indicate ground surface uplift; ND = Not determined due to lateral spreading; NA = Not available due to the absence of the Sep-2010 LiDAR survey.

Table 7: Corrected liquefaction-related ground surface subsidence for Patches A, B, and C using LiDAR DEMs.

	Estimated Ground Surface Subsidence (mm)								
	10-m Buffer			20-m Buffer			50-m Buffer		
Earthquake Event(s)	16th %ile	50th %ile	84th %ile	16th %ile	50th %ile	84th %ile	16th %ile	50th %ile	84th %ile
Sep-10	NA	NA	NA	NA	NA	NA	NA	NA	NA
Feb-11	ND	ND	ND	ND	ND	ND	ND	ND	ND
Jun-11	ND	ND	ND	ND	ND	ND	ND	ND	ND
Dec-11	ND	ND	ND	ND	ND	ND	ND	ND	ND
CES	ND	ND	ND	ND	ND	ND	ND	ND	ND

Notes: NA = Not available due to the absence of the Sep-10 lidar survey; ND = Not determined due to lateral spreading.

Note 2: Comparison between the ground surface subsidence based on original LiDAR survey points and the ground surface subsidence based on LiDAR DEMs is not available for the Sep-10 (and Feb-10) earthquake(s) because the September-10 LiDAR survey did not capture the ground surface elevation at the site. The ground surface subsidence was not determined for the Feb-11, Jun-11, and Dec-11 earthquakes and the CES due to lateral spreading.

Table 8a: Ejecta-Induced settlement for the top 20 m of the soil profile for Patch A for the 50th %ile PGA, P_L=50%, and C_{FC}=0.13 using BI-2014, ZRB-2002, and I_C cutoff of 2.6.

Earthquake Event(s)	M_W	PGA (g)	Depth to Groundwater (m)	S_T (mm)	S_{V1D}* (mm)	$S_{E,L}$ (mm)
Sep-10	7.1	0.21	1.5	NA	32±20	NA
Feb-11	6.2	0.34	1.5	ND	ND	ND
Jun-11	6.2	0.17	1.2	ND	ND	ND
Dec-11	6.1	0.18	1.2	ND	ND	ND

Notes: S_T = Total settlement (Table 6); S_{V1D} = Average vertical settlement due to volumetric compression using Boulanger and Idriss (2014) (BI-2014), Zhang et al. (2002) (ZRB-2002) procedures and de Greef and Lengkeek (2018) thin-layer correction; $S_{E,L}$ = Ejecta-induced settlement as the difference between the LiDAR-based S_T and S_{V1D}; ND = Not determined due to lateral spreading; NA= Not available due to the absence of the Sep-2010 LiDAR survey; *S_{V1D} was computed for the available CPT trace (tip refusal at ~6-7 m below ground surface due to gravel).

Table 8b: Ejecta-Induced settlement for the top 20 m of the soil profile for Patch B for the 50th %ile PGA, P_L=50%, and C_{FC}=0.13 using BI-2014, ZRB-2002, and I_C cutoff of 2.6.

Earthquake Event(s)	M_W	PGA (g)	Depth to Groundwater (m)	S_T (mm)	S_{V1D} (mm)	$S_{E,L}$ (mm)
Sep-10	7.1	0.21	1.5	NA	39±20	NA
Feb-11	6.2	0.34	1.5	ND	ND	ND
Jun-11	6.2	0.17	1.2	ND	ND	ND
Dec-11	6.1	0.18	1.2	ND	ND	ND

Notes: S_T = Total settlement (Table 6); S_{V1D} = Average vertical settlement due to volumetric compression using Boulanger and Idriss (2014) (BI-2014), Zhang et al. (2002) (ZRB-2002) procedures and de Greef and Lengkeek (2018) thin-layer correction; $S_{E,L}$ = Ejecta-induced settlement as the difference between the LiDAR-based S_T and S_{V1D}; ND = Not determined due to lateral spreading; NA= Not available due to the absence of the Sep-2010 LiDAR survey; *S_{V1D} was computed for the available CPT trace (tip refusal at ~6-7 m below ground surface due to gravel).

Table 8c: Ejecta-Induced settlement for the top 20 m of the soil profile for Patch C for the 50th %ile PGA, P_L=50%, and C_{FC}=0.13 using BI-2014, ZRB-2002, and I_C cutoff of 2.6.

Earthquake Event(s)	M_W	PGA (g)	Depth to Groundwater (m)	S_T (mm)	S_{V1D} (mm)	$S_{E,L}$ (mm)
Sep-10	7.1	0.21	1.5	NA	26±20	NA
Feb-11	6.2	0.34	1.5	ND	ND	ND
Jun-11	6.2	0.17	1.2	ND	ND	ND
Dec-11	6.1	0.18	1.2	ND	ND	ND

Notes: S_T = Total settlement (Table 6); S_{V1D} = Average vertical settlement due to volumetric compression using Boulanger and Idriss (2014) (BI-2014), Zhang et al. (2002) (ZRB-2002) procedures and de Greef and Lengkeek (2018) thin-layer correction; $S_{E,L}$ = Ejecta-induced settlement as the difference between the LiDAR-based S_T and S_{V1D}; ND = Not determined due to lateral spreading; NA= Not available due to the absence of the Sep-2010 LiDAR survey; *S_{V1D} was computed for the available CPT trace (tip refusal at ~6-7 m below ground surface due to gravel).

Note 3: The uncertainty for volumetric settlement was derived based on the sensitivity of volumetric settlement to PGA, C_{FC}, and P_L for each earthquake event for VsVp 57203 *Shirley Intermediate School* and CC LIQ 1 – CPT 5586 – *Vivian St* sites. Taking the 50th percentile as the baseline case, the minimum and maximum values corresponding to the difference between the 25th percentile and the 50th percentile and the 75th percentile and the 50th percentile were determined. The arithmetic mean of the range of the minimum and maximum difference was evaluated for each patch at the two sites. The maximum arithmetic mean for each earthquake event was rounded to the nearest five and used as the uncertainty value. Accordingly, the 1-D volumetric settlement uncertainties of ±20, ±50, ±25, and ±50 mm for the Sep-10, Feb-11, Jun-11, and Dec-11 earthquake events, respectively, were used for all sites in this study.

Table 9a: Coverage area and height of ejecta estimates for Patch A (10-, 20-, and 50-m buffers) using photographs.

Earthquake Event	$A_{E,thick}$ (m^2)	$H_{E,thick}$ (mm)	$A_{E,thin}$ (m^2)	$H_{E,thin}$ (mm)	A_T (m^2)
Sep-10	0	0	0	0	31.9
Feb-11	ND	ND	ND	ND	31.9
Jun-11	ND	ND	ND	ND	31.9
Dec-11	ND	ND	ND	ND	31.9

Notes: $A_{E,thick/thin}$ = Coverage area of thick/thin ejecta layers; $H_{E,thick/thin}$ = Lower-upper estimate of height of thick/thin ejecta layers; A_T = Total assessment area of a buffer being considered; Thin and thick layers correspond to light gray and dark gray colors of ejecta observed in aerial photographs; ND = Not determined due to lateral spreading.

Table 9b: Coverage area and height of ejecta estimates for Patch B (50-m buffer) using photographs.

Earthquake Event	$A_{E,thick}$ (m^2)	$H_{E,thick}$ (mm)	$A_{E,thin}$ (m^2)	$H_{E,thin}$ (mm)	A_T (m^2)
Sep-10	0	0	0	0	48.4
Feb-11	ND	ND	ND	ND	48.4
Jun-11	ND	ND	ND	ND	48.4
Dec-11	ND	ND	ND	ND	48.4

Notes: $A_{E,thick/thin}$ = Coverage area of thick/thin ejecta layers; $H_{E,thick/thin}$ = Lower-upper estimate of height of thick/thin ejecta layers; A_T = Total assessment area of a buffer being considered; Thin and thick layers correspond to light gray and dark gray colors of ejecta observed in aerial photographs; ND = Not determined due to lateral spreading.

Table 9c: Coverage area and height of ejecta estimates for Patch C (50-m buffer) using photographs.

Earthquake Event	$A_{E,thick}$ (m^2)	$H_{E,thick}$ (mm)	$A_{E,thin}$ (m^2)	$H_{E,thin}$ (mm)	A_T (m^2)
Sep-10	0	0	0	0	78.1
Feb-11	ND	ND	ND	ND	78.1
Jun-11	ND	ND	ND	ND	78.1
Dec-11	ND	ND	ND	ND	78.1

Notes: $A_{E,thick/thin}$ = Coverage area of thick/thin ejecta layers; $H_{E,thick/thin}$ = Lower-upper estimate of height of thick/thin ejecta layers; A_T = Total assessment area of a buffer being considered; Thin and thick layers correspond to light gray and dark gray colors of ejecta observed in aerial photographs; ND = Not determined due to lateral spreading.

Note 4: The Sep-10 ejecta-induced settlement values in Table 9 are based on the satellite images of the site (Figures 8 and 9) showing no ejecta and the Cubrinovski et al. (2011)[3] liquefaction map. The ejecta-induced settlement using photographs and engineering judgment, $S_{E,P}$, is estimated as

$$S_{E,P} = \frac{\sum_{i=1}^{a} A_{E,thick,i} * H_{E,thick,i} + \sum_{j=1}^{b} A_{E,thin,j} * H_{E,thin,j}}{A_T} = \frac{\sum_{i=1}^{a} V_{E,thick,i} + \sum_{j=1}^{b} V_{E,thin,j}}{A_T}$$

where

- $A_{E,thick,i}$ and $H_{E,thick,i}$ are the area and the height of a thick ejecta layer, respectively;
- $A_{E,thin,j}$ and $H_{E,thin,j}$ are the area and the height of a thin ejecta layer, respectively;
- A_T is the total assessment area for a buffer being considered (Figure 1).

Table 10: Ejecta-induced settlement estimates for Patches A, B, and C based on photographs.

Earthquake Event	Patch A (10-, 20-, and 50-m buffers)		Patch B (50-m buffer)		Patch C (50-m buffer)	
	$S_{E,P,lower}$ (mm)	$S_{E,P,upper}$ (mm)	$S_{E,P,lower}$ (mm)	$S_{E,P,upper}$ (mm)	$S_{E,P,lower}$ (mm)	$S_{E,P,upper}$ (mm)
Sep-10	0	0	0	0	0	0
Feb-11	ND	ND	ND	ND	ND	ND
Jun-11	ND	ND	ND	ND	ND	ND
Dec-11	ND	ND	ND	ND	ND	ND

Notes: $S_{E,P,lower}$ and $S_{E,P,upper}$ correspond to lower and upper estimates of $S_{E,P}$, respectively; ND = Not determined due to lateral spreading.

Table 11: Best final estimates of ejecta-induced settlement for Patches A, B, and C.

EQ Event	Patch A (10-, 20-, and 50-m buffers)			Patch B Patch B (50-m buffer)			Patch C (50-m buffer)		
	$S_{E,L}$ (mm)	$S_{E,P}$ (mm)	$S_{E,final}$ (mm)	$S_{E,L}$ (mm)	$S_{E,P}$ (mm)	$S_{E,final}$ (mm)	$S_{E,L}$ (mm)	$S_{E,P}$ (mm)	$S_{E,final}$ (mm)
Sep-10	NA	0	0	NA	0	0	NA	0	0
Feb-11	ND	ND	ND	ND	ND	ND	ND	ND	ND
Jun-11	ND	ND	ND	ND	ND	ND	ND	ND	ND
Dec-11	ND	ND	ND	ND	ND	ND	ND	ND	ND

Notes: $S_{E,L}$ = Ejecta-induced settlement based on LiDAR data reported in Table 8; $S_{E,P}$ = Median ejecta-induced settlement for the range of values reported in Table 10; $S_{E,final}$ = Best final estimate of ejecta-induced settlement rounded to the nearest 5; Final plus/minus values are also rounded to the nearest 5; ND = Not determined due to lateral spreading; NA= Not available due to the absence of the Sep-2010 LiDAR survey.

[3] Cubrinovski, M., Bradley, B., Wotherspoon, L., Green, R., Bray, J., Wood, C., … Wells, D. (2011). Geotechnical aspects of the 22 February 2011 Christchurch earthquake. *Bulletin of the New Zealand Society for Earthquake Engineering, 44*(4), 205-226. doi:10.5459/bnzsee.44.4.205-226

Note 5:

- $S_{E,final}$ for Patches A, B, and C is based solely on $S_{E,P}$ for the Sep-10 earthquake.
- $S_{E,final}$ for the Feb-10, Jun-11, and Dec-11 earthquakes was not determined due to lateral spreading that started with the Feb-11 earthquake.
- The site is in the zone of moderate to severe LPI overprediction of liquefaction severity for the Sep-10 earthquake (as well as the Feb-11 earthquake), according to Maurer et al. (2019)[4].

Summary:

The best estimate of the ejecta-induced free-field ground settlement at the 15b Royds Pl site for the SEP 2010 earthquake is 0 mm. For the FEB 2011, JUN 2011, and DEC 2011 earthquake, the ejecta-induced free-field settlement was not determined due to lateral spreading.

Figure 2: Location of the site.

[4] Maurer, B. W., Green, R. A., Cubrinovski, M., & Bradley, B. A. (2014). Evaluation of the Liquefaction Potential Index for Assessing Liquefaction Hazard in Christchurch, New Zealand. *Journal of Geotechnical and Geoenvironmental Engineering*, 140(7), 04014032-1-11. doi:10.1061/(asce)gt.1943-5606.0001117

Figure 3: Position of the site relative to nearby buildings, vegetation, and free-face features.

Figure 4: Ground photographs of slightly sloping ground near and toward the stream. The photograph on the right also shows the step change in the ground surface due to the stream.

Figure 5: Satellite image of the site taken in Apr 2004.

Figure 6: Satellite image of the site taken in Mar 2009.

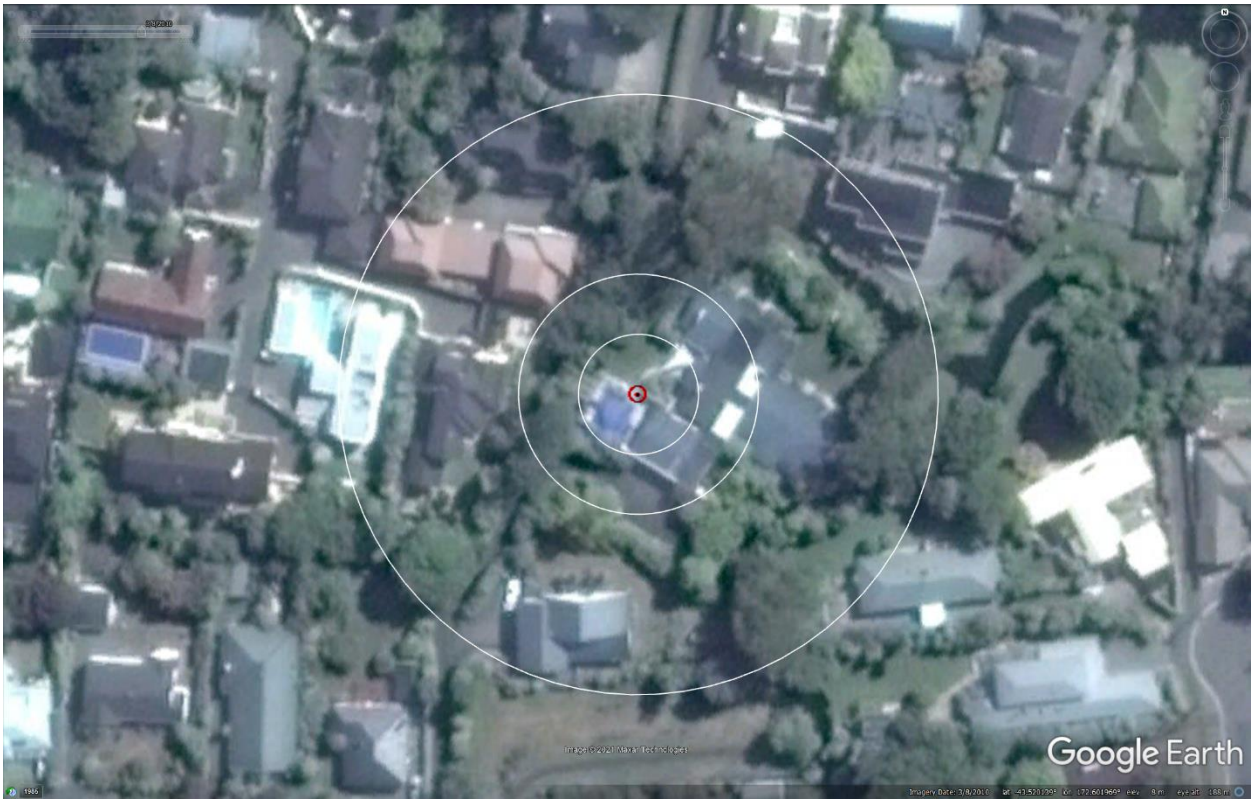

Figure 7: Satellite image of the site taken in Mar 2010.

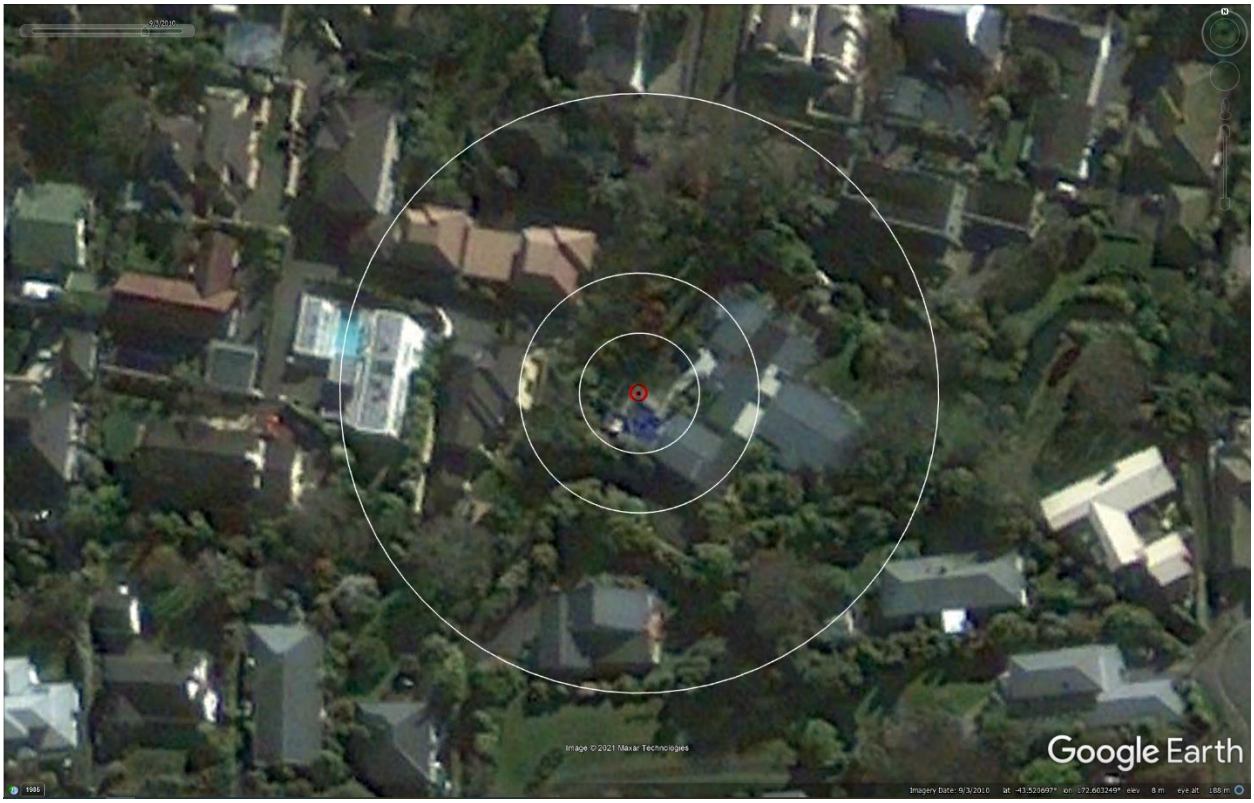

Figure 8: Satellite image of the site taken on 3 Sep 2010.

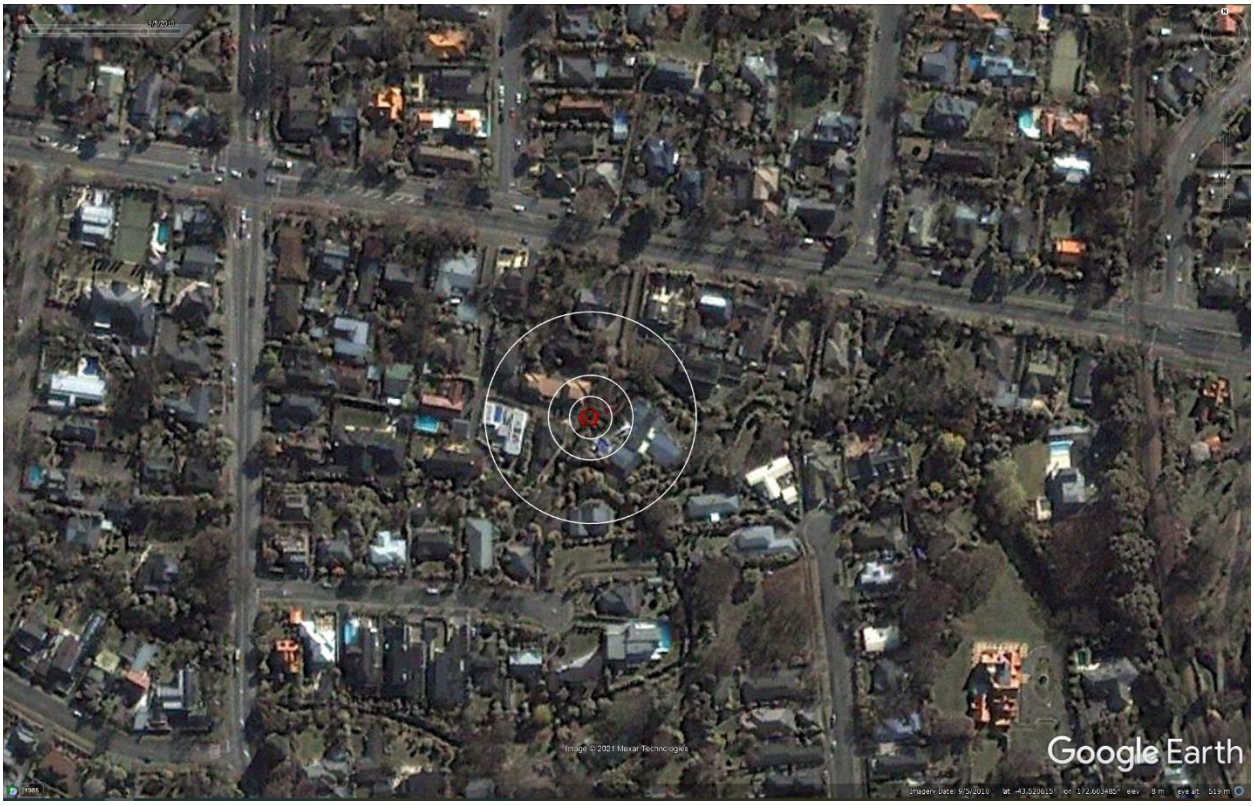

Figure 9: Satellite image of the site taken on 5 Sep 2010.

Figure 10: Satellite image of the site taken on 7 Feb 2010.

Figure 11: No aerial photograph of the site from Sep 4, 2010.

Figure 12: Aerial photograph of the site taken on Feb 24, 2011.

Figure 13: No aerial photograph of the site from June 14-15, 2011.

Figure 14: Aerial photograph of the site taken on June 16, 2011.

Figure 15: Aerial photograph of the site taken on Dec 24, 2011.

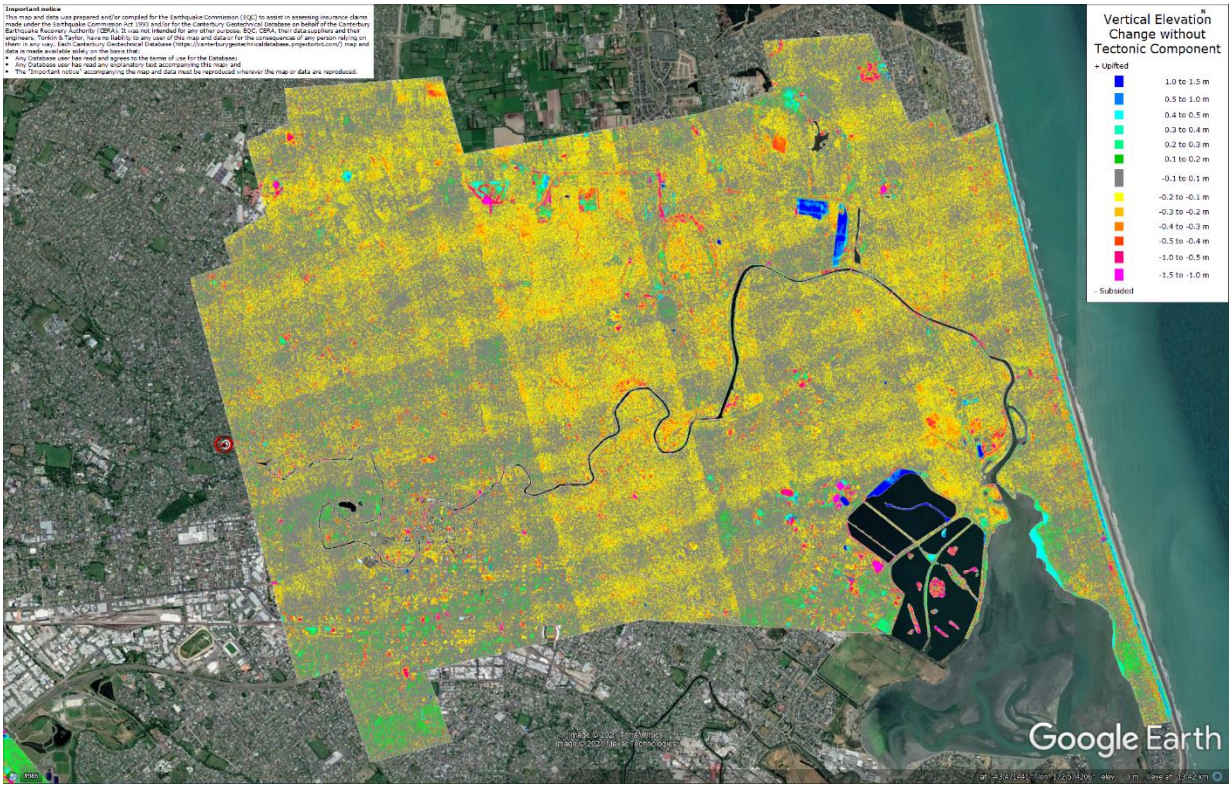

Figure 16: Vertical Ground Movements (Surface – Tectonic) for Sep 2010 Earthquake were not captured due to the absence of Sep 2010 LiDAR survey.

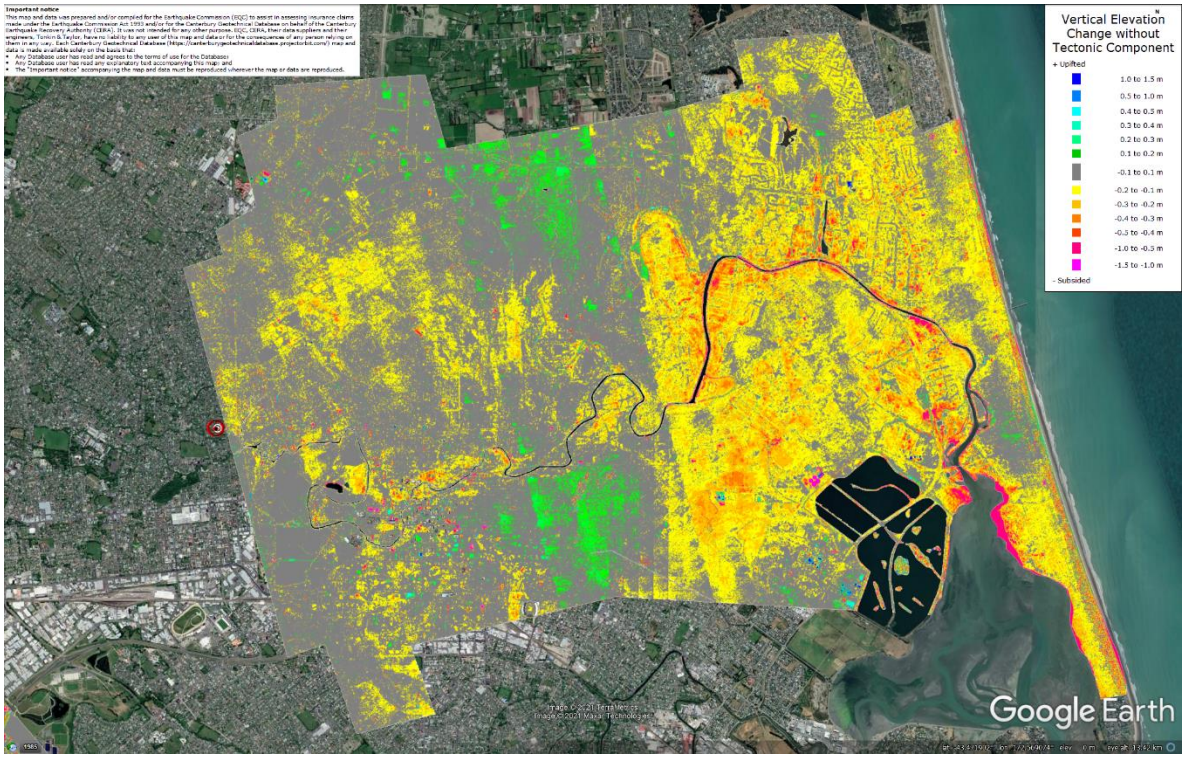

Figure 17: Vertical Ground Movements (Surface – Tectonic) for Feb 2011 Earthquake were not captured due to the absence of Sep 2010 LiDAR survey.

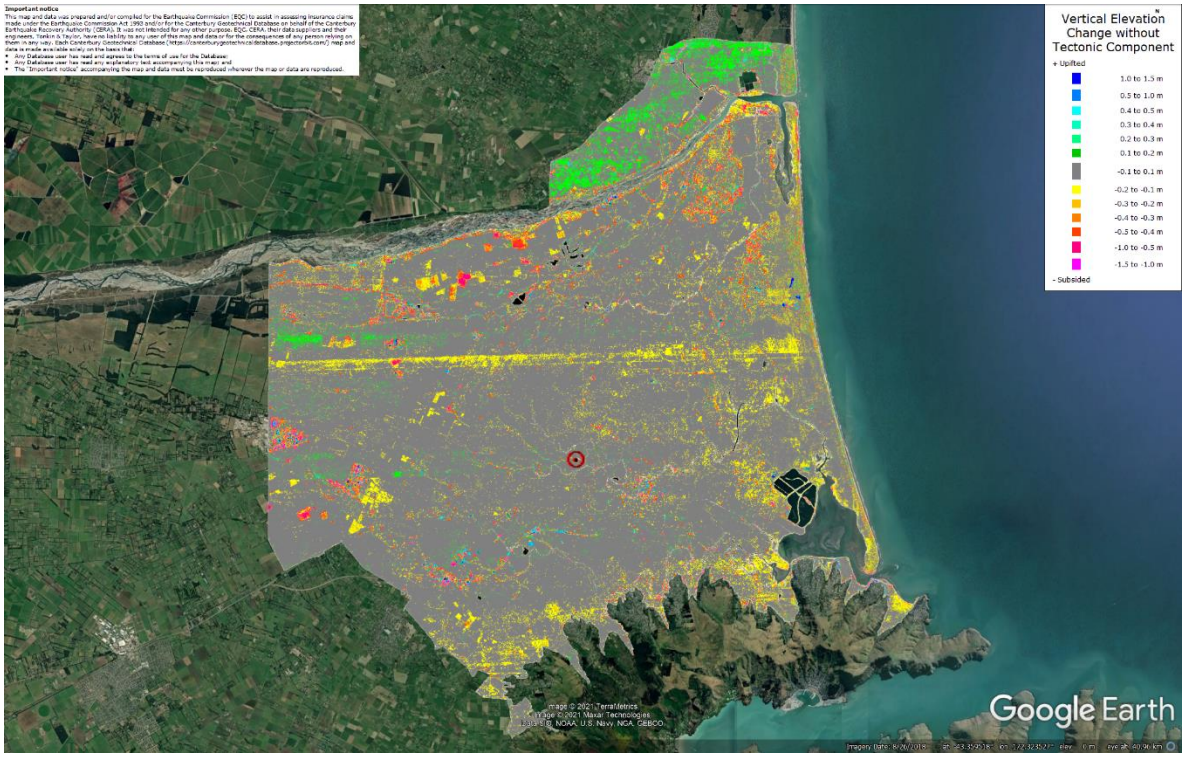

Figure 18: Vertical Ground Movements (Surface – Tectonic) for June 2011 Earthquake – the site is not in the apparent zone of overestimated or underestimated ground surface subsidence.

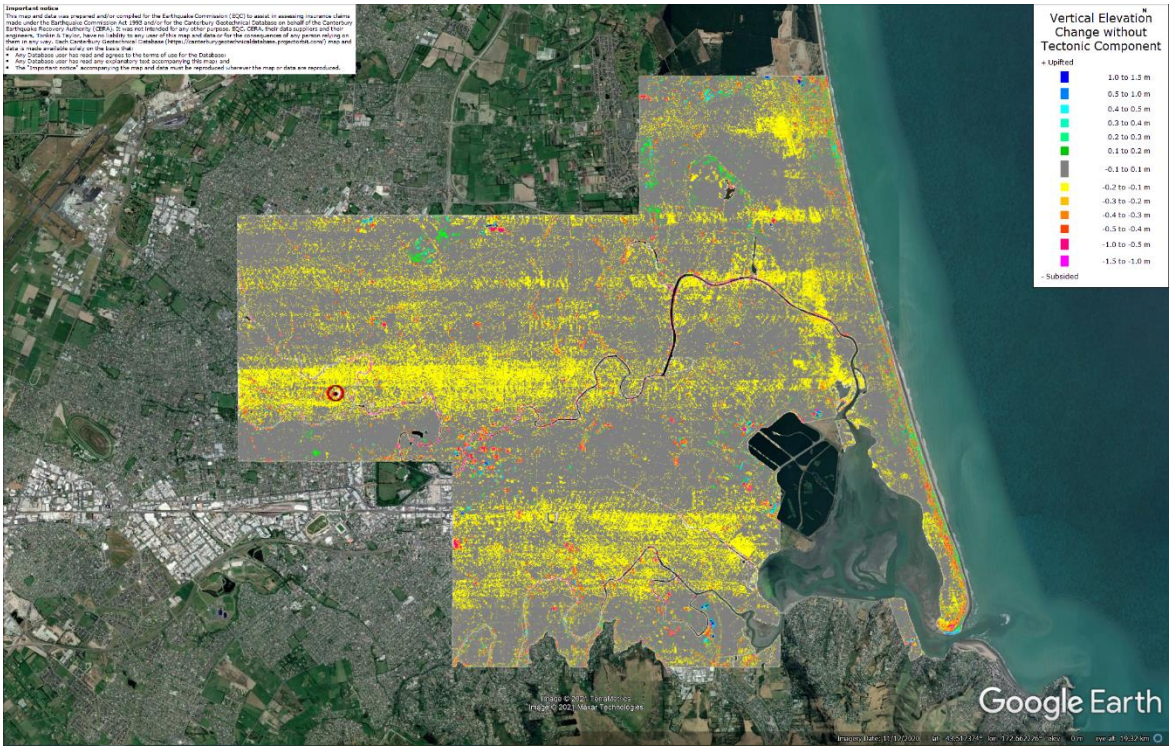

Figure 19: Vertical Ground Movements (Surface – Tectonic) for Dec 2011 Earthquake – the site is in the apparent zone of overestimated ground surface subsidence due to the underestimated ground surface elevation by the Oct 2012 LiDAR survey.

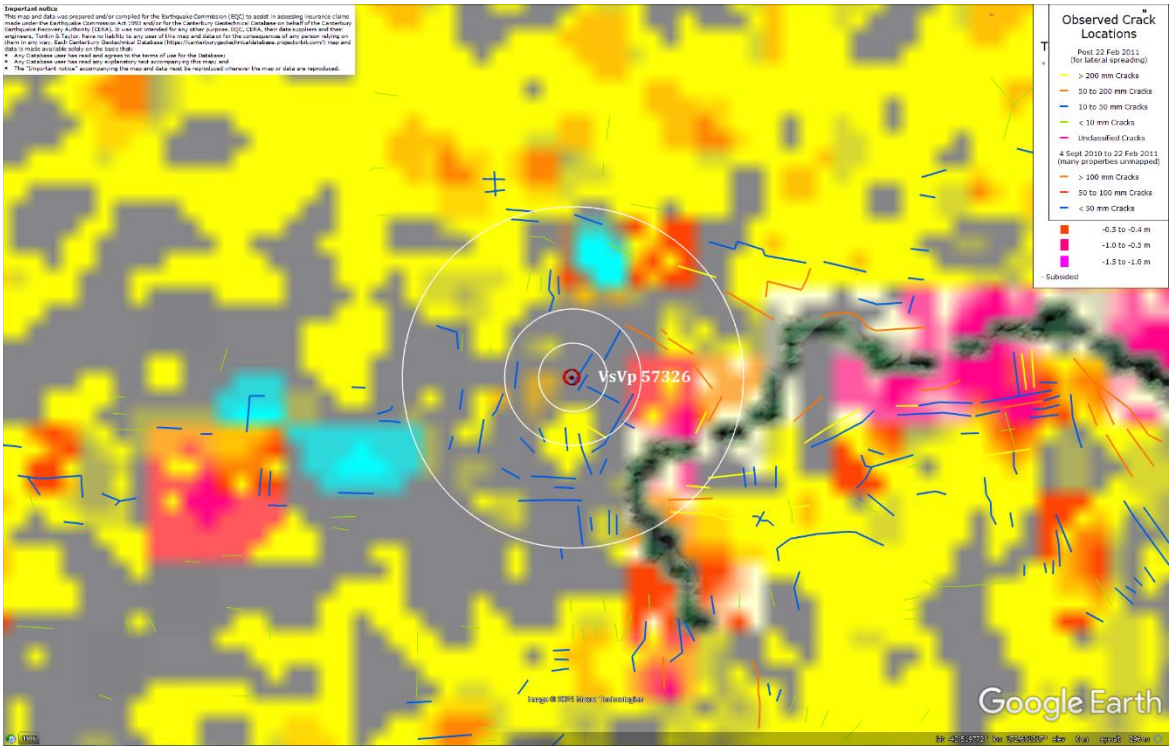

Figure 20: Lateral spreading for Canterbury Earthquake Sequence (no lateral spreading for Sep-10 EQ but Feb-11 EQ).

Figure 21: Vertical tectonic movements for Sep 2010 Earthquake.

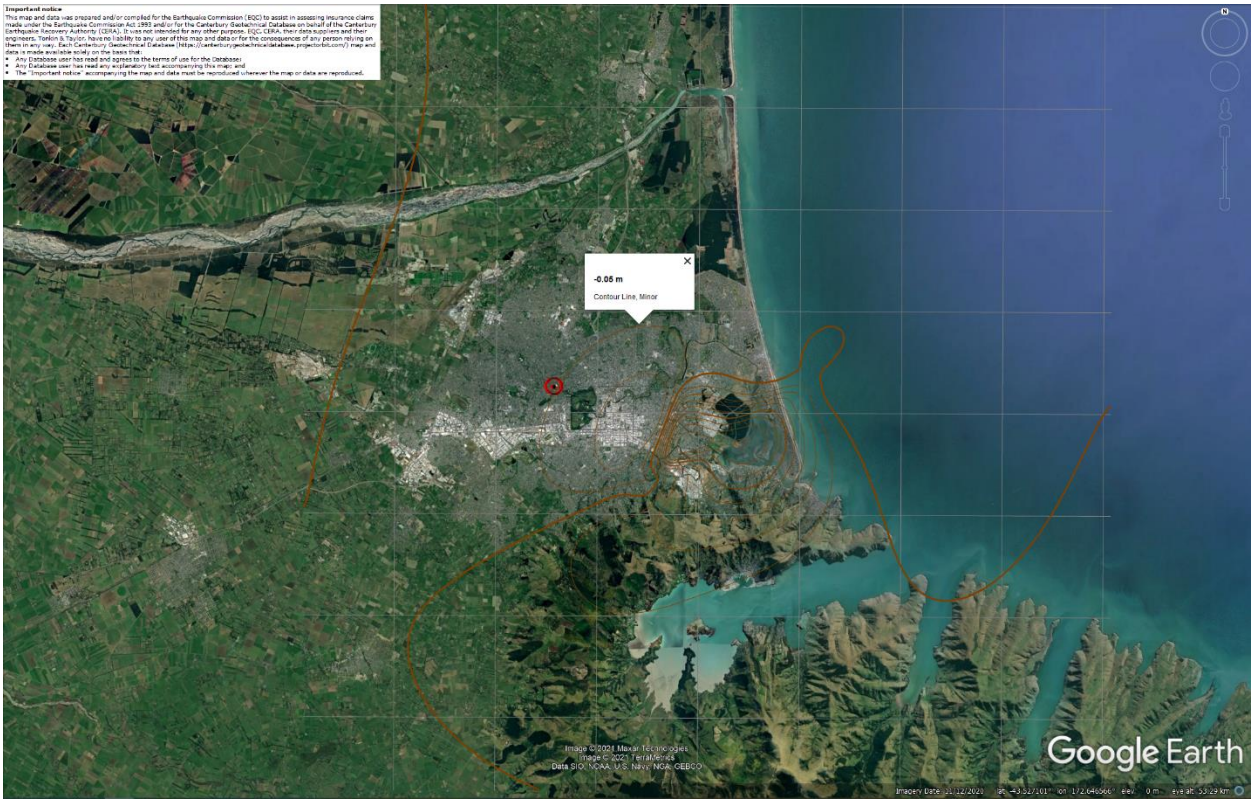

Figure 22: Vertical tectonic movements for Feb 2011 Earthquake.

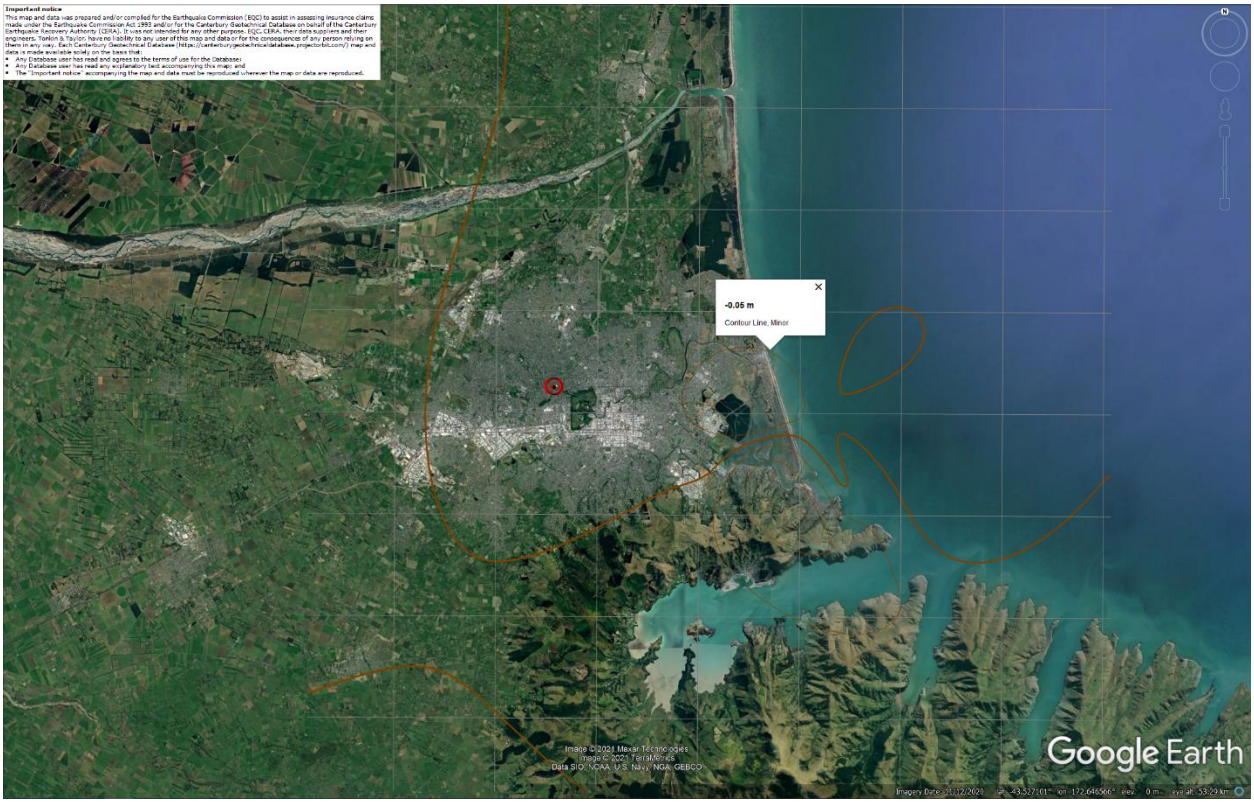

Figure 23: Vertical tectonic movements for June 2011 Earthquake.

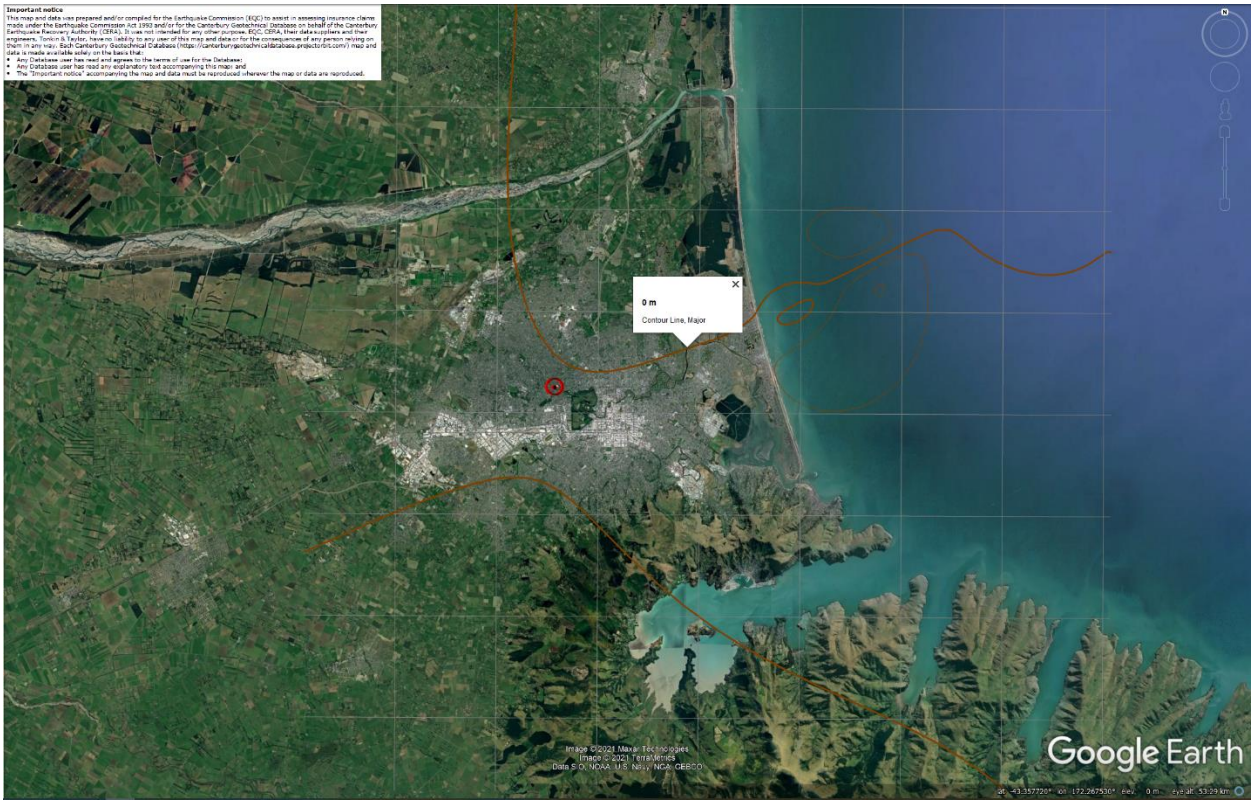

Figure 24: Vertical tectonic movements for Dec 2011 Earthquake.

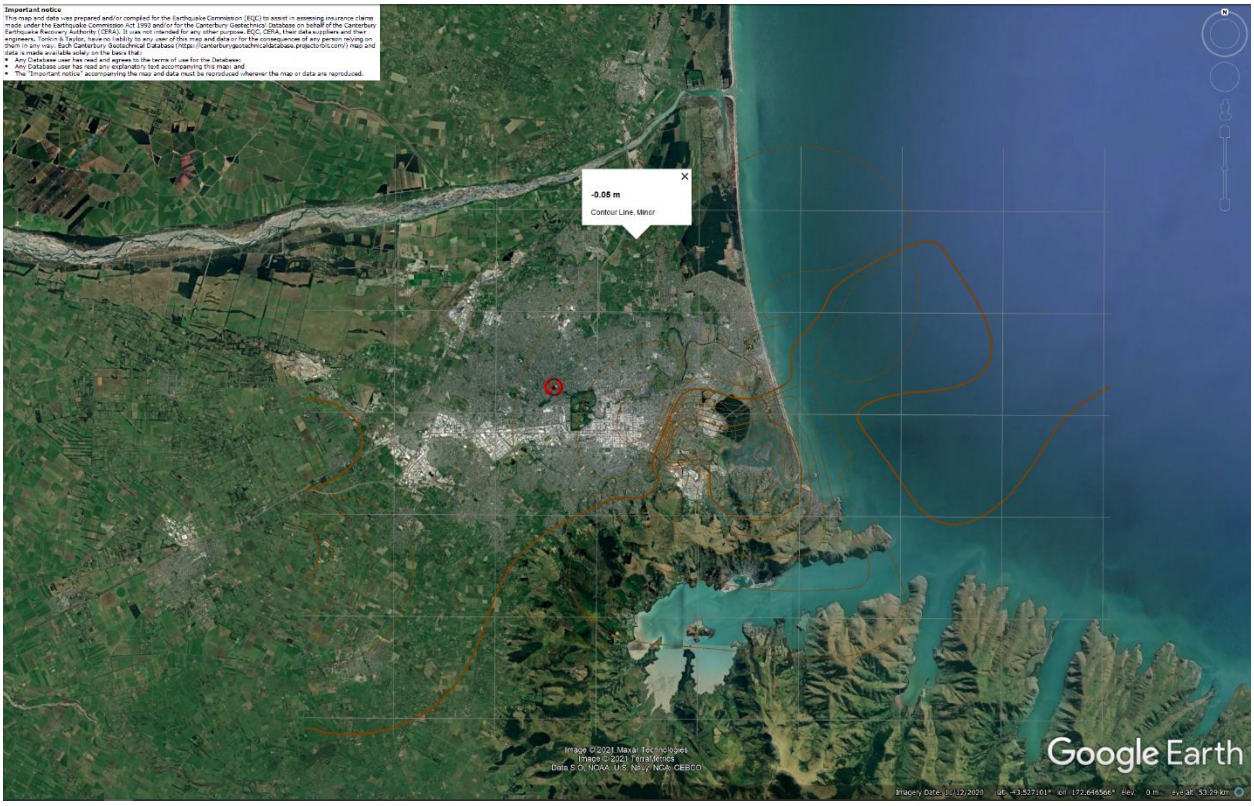

Figure 25: Vertical tectonic movements for Canterbury Earthquake Sequence.

Figure 26: PGA for Sep-10 EQ (st. dev. = 0.325-0.350 ln units).

Figure 27: PGA for Feb-11 EQ (st. dev. = 0.350-0.375 ln units).

Figure 28: PGA for Jun-11 EQ (st. dev. = 0.375-0.400 ln units).

Figure 29: PGA for Dec-11 EQ (st. dev. = 0.375-0.400 ln units).

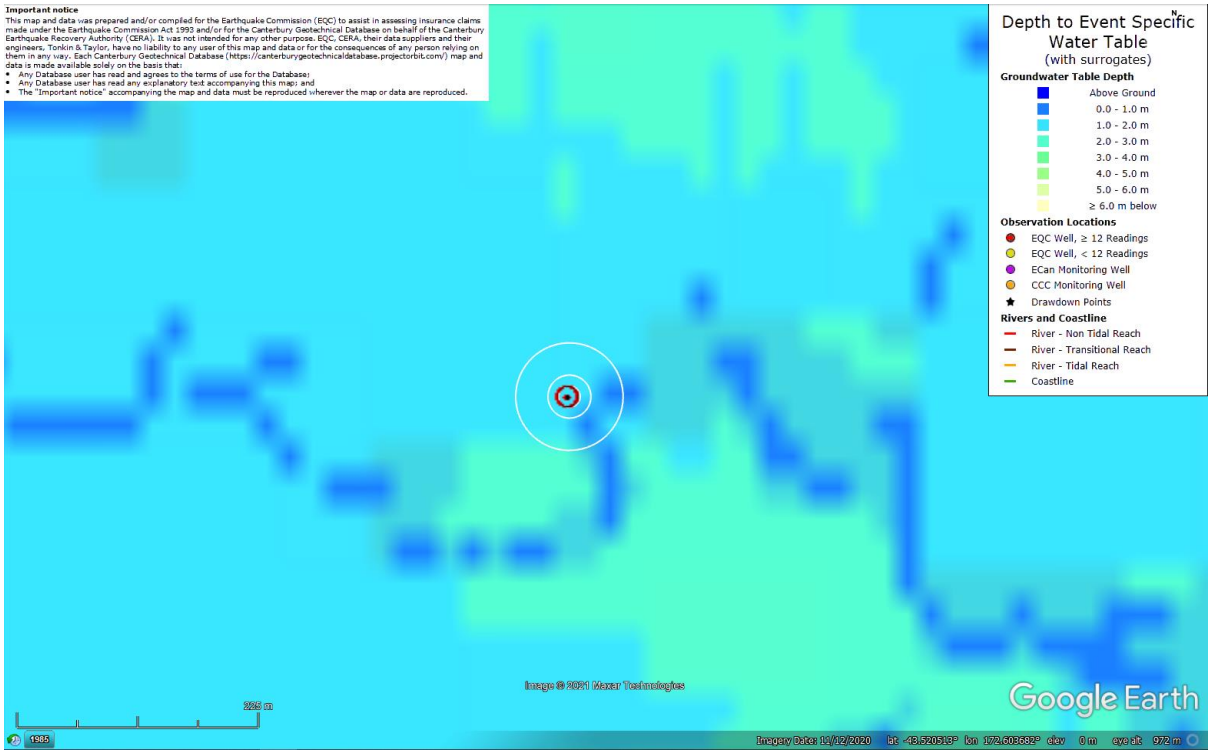

Figure 30: Depth to groundwater table for Sep-10 EQ.

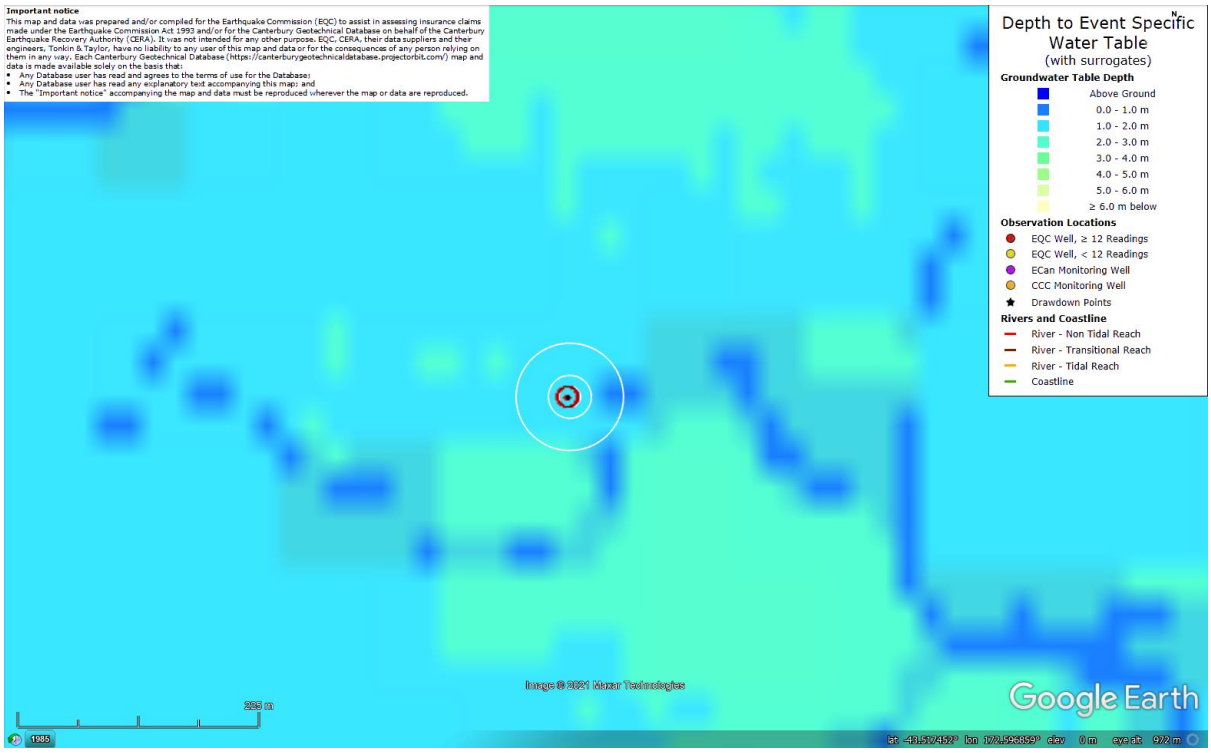

Figure 31: Depth to groundwater table for Feb-11 EQ.

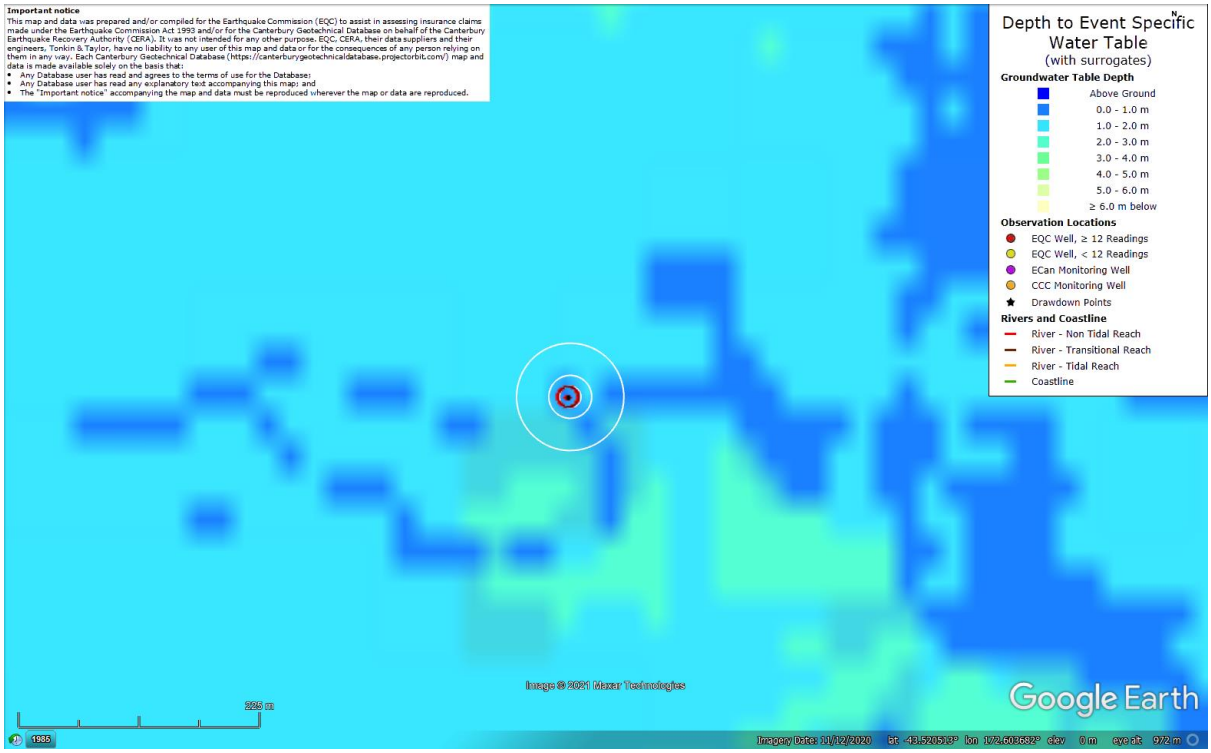

Figure 32: Depth to groundwater table for Jun-11 EQ.

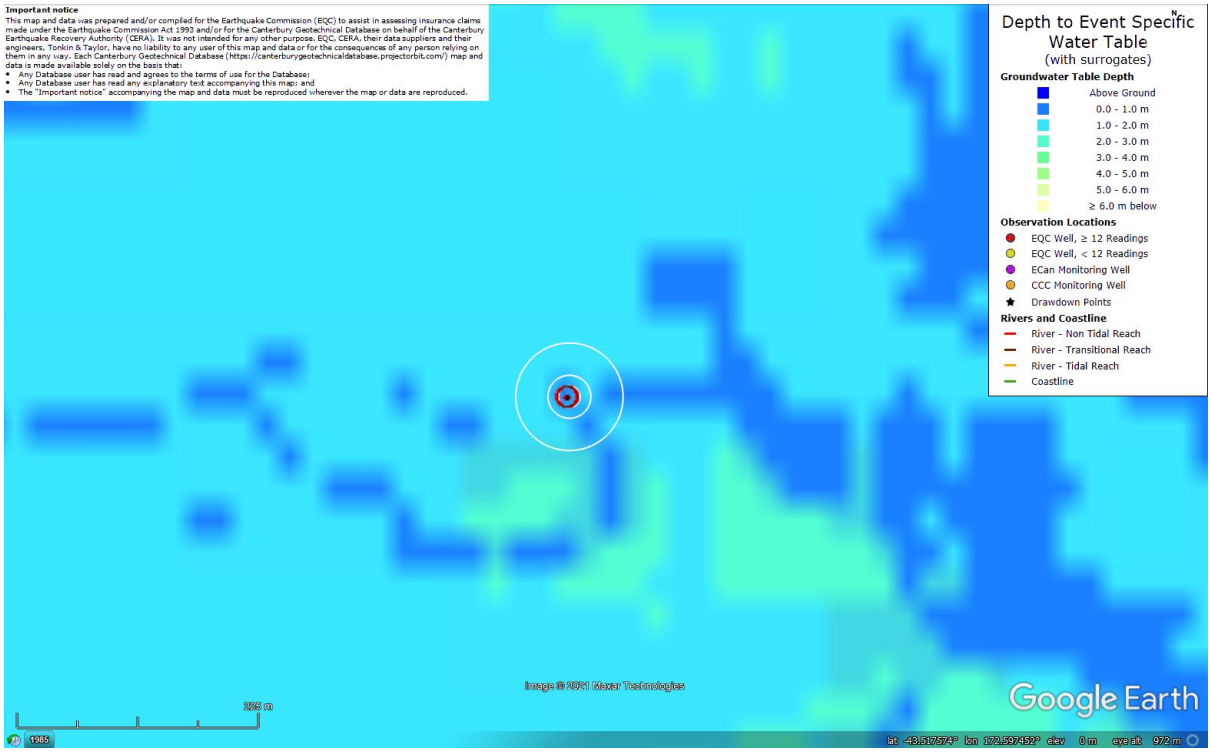

Figure 33: Depth to groundwater table for Dec-11 EQ.

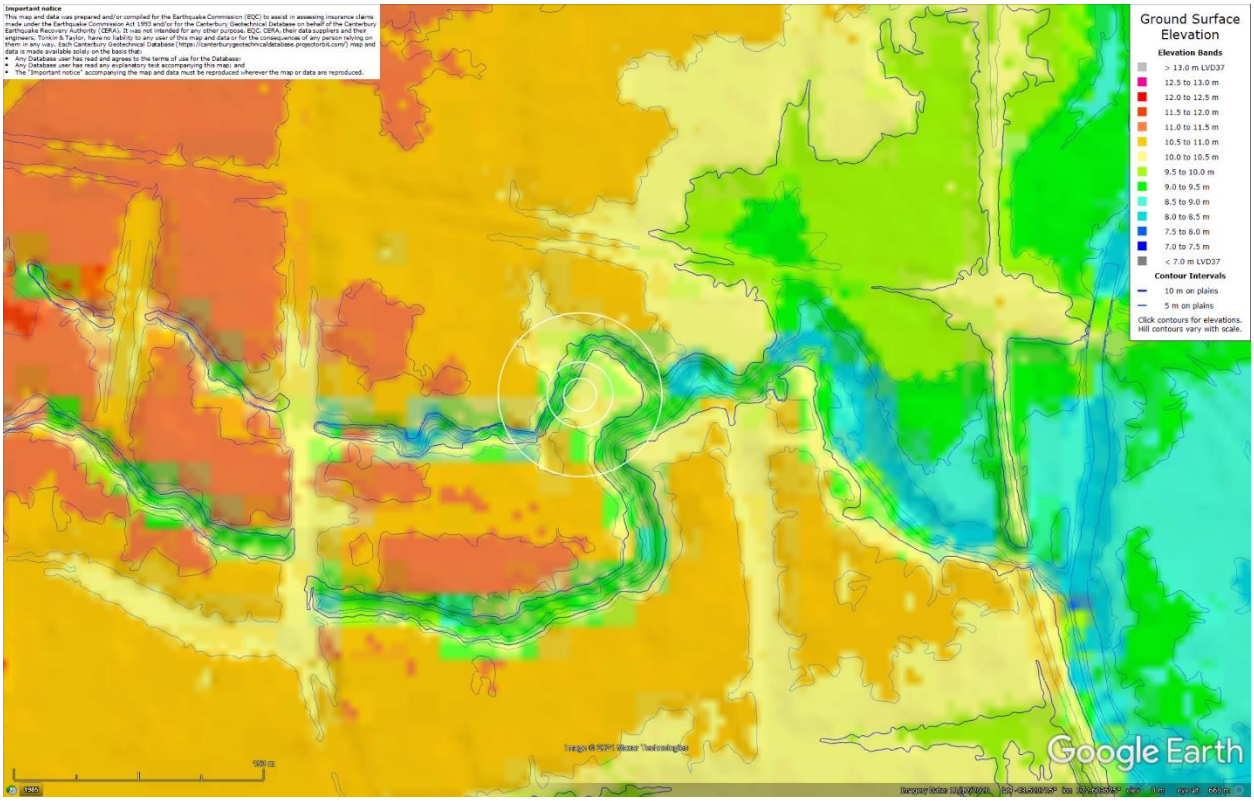

Figure 34: Ground surface elevation according to the Sep-11 LIDAR survey.

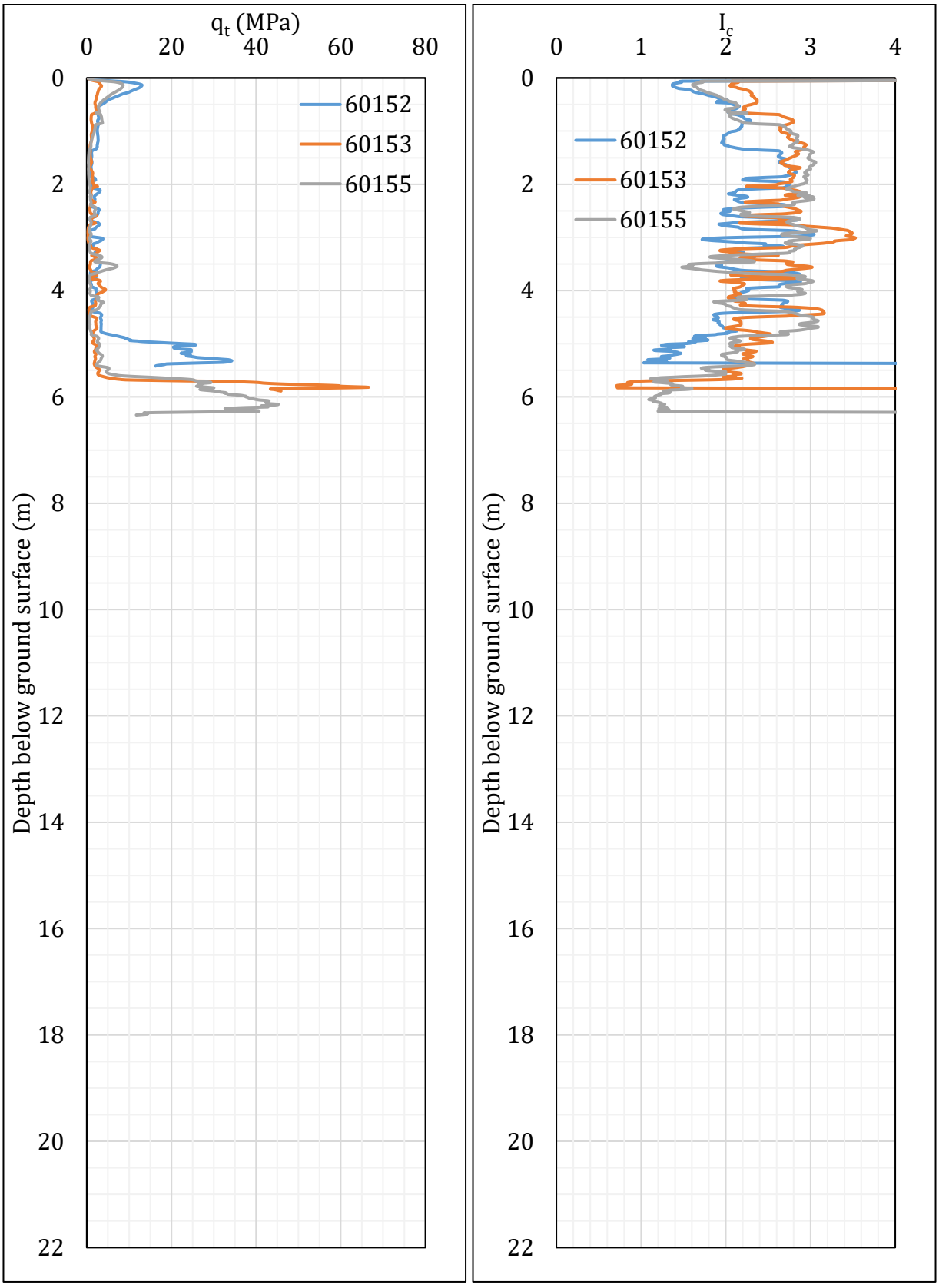

Figure 35: q_t and I_c profiles.

Note 6: The selection of CPTs for the area considered for settlement assessment (Figure 1) is based on the proximity of the CPTs to the considered areas. In accordance with that, the following table shows CPTs that were used for the volumetric settlement analysis in *Cliq v.3.0.3.2*, a CPT soil liquefaction software developed by GeoLogismiki. (The average volumetric settlements were reported in Table 8.)

Table 12: CPT profiles used in volumetric settlement analysis for areas selected for settlement assessment.

CPT ID No.	Patch A	Patch B	Patch C
60152	✓	✓	
60153		✓	
60155			✓

Table 13: CPT-based results.

		CPT ID		
EQ Event	Parameter	60152	60153	60155
Sep-10	S_{V1D} (mm)	35	49	30
	LSN	10	11	7
	LPI	2	3	2
	LPI_{ish}	0	2	0
	$D_{FS<1}$ (m)	3.19	4.05	2.41
Feb-11	S_{V1D} (mm)	ND	ND	ND
	LSN	ND	ND	ND
	LPI	ND	ND	ND
	LPI_{ish}	ND	ND	ND
	$D_{FS<1}$ (m)	ND	ND	ND
Jun-11	S_{V1D} (mm)	ND	ND	ND
	LSN	ND	ND	ND
	LPI	ND	ND	ND
	LPI_{ish}	ND	ND	ND
	$D_{FS<1}$ (m)	ND	ND	ND
Dec-11	S_{V1D} (mm)	ND	ND	ND
	LSN	ND	ND	ND
	LPI	ND	ND	ND
	LPI_{ish}	ND	ND	ND
	$D_{FS<1}$ (m)	ND	ND	ND

Notes: $D_{FS<1}$ = Depth to the first liquefiable layer ($FS_L<1$) that is at least 200-mm thick, as determined by the Boulanger and Idriss (2016) liquefaction-triggering procedure (P_L=50%, C_{FC}=0.13, and $I_{c,cutoff}$ =2.6), and exported from *Cliq v.3.0.3.2*; undet. = the specified soil layer was not detected; Negligible settlement is assumed for a depth range from ~6 m to 20 m.

Note 7: Based on the borehole log (BH 18056, Figure 1), the groundwater table is at a depth of 1.3 m below the ground surface. The soil profile consists of (1) sandy fine to coarse gravel, GW, fill below asphalt to a depth of 0.3 m, (2) silt, ML, of the Springston formation (Yaldhurst member, alluvial) to a depth of 3.3 m, (3) fine to medium sand, SP, of the Springston formation (Yaldhurst member, alluvial) to a depth of 4.4 m, (4) silt, ML, of the Springston formation (Yaldhurst member, alluvial) to a depth of 5.0 m, (5) fine to medium sand, SP, of the Springston formation (Yaldhurst member, alluvial) to a depth of 6.2 m, (6) fine to coarse gravel, GW, of the Springston formation (Yaldhurst member, alluvial) to a depth of 9.0 m, (7) fine to coarse sand, SP, of the Springston formation (Yaldhurst member, alluvial) to a depth of 9.45 m, (8) fine to coarse gravel, GW, of the Springston formation (Yaldhurst member, alluvial) to a depth of 13.55 m, (9) silt, ML, of the Christchurch formation (marine/estuarine) to a depth of 14.8 m, (10) silty fine to medium sand, SM, of the Christchurch formations (marine/estuarine) to a depth of 16.0 m, (11) silt, ML, of the Christchurch formation (marine/estuarine) to a depth of 16.55 m, (12) fine to coarse sand, SW, of the Christchurch formation (marine/estuarine) to a depth of 16.95 m, and (13) fine to coarse Riccarton gravel, GW, to a depth of 20 m (the end of the borehole).